Photothermal behavior for two-dimensional nanoparticle ensembles: Multiple scattering and thermal accumulation effects

Minggang Luo,[1,2] Junming Zhao,[1,3,*] Linhua Liu,[4] and Mauro Antezza[2,5,†]

[1]*School of Energy Science and Engineering, Harbin Institute of Technology, 92 West Street, Harbin 150001, China*
[2]*Laboratoire Charles Coulomb (L2C), UMR 5221, CNRS-Université de Montpellier, F-34095 Montpellier, France*
[3]*Key Laboratory of Aerospace Thermophysics, Ministry of Industry and Information Technology, Harbin 150001, China*
[4]*School of Energy and Power Engineering, Shandong University, Qingdao 266237, China*
[5]*Institut Universitaire de France, 1 rue Descartes, F-75231 Paris Cedex 5, France*

(Received 12 October 2021; revised 8 April 2022; accepted 6 June 2022; published 23 June 2022)

Light-assisted micronanoscale temperature control in a complex nanoparticle network has attracted a lot of research interest. Many efforts have been put into the optical properties of nanoparticle networks, and only a few investigations have reported its light-induced thermal behavior. We consider a two-dimensional (2D) square-lattice nanoparticle ensemble made of typical metal Ag with a radius of 5 nm. The effect of complex multiple scattering and thermal accumulation on light-induced thermal behavior in plasmonic resonance frequency (around 383 nm) is analyzed through the Green's function approach. The regime borders of both multiple scattering and thermal accumulation effects on the photothermal behavior of the 2D square-lattice nanoparticle ensemble are figured out clearly and quantitatively. The dimensionless parameter φ is defined as the ratio of a full temperature increase to that without considering the multiple scattering or thermal accumulation to quantify the multiple scattering and thermal accumulation effects on photothermal behavior. The more compact the nanoparticle ensemble is, the stronger the multiple scattering effect on thermal behavior is. When the lattice spacing increases to dozens times of the radius, the multiple scattering becomes insignificant. When $\varphi \approx 1$ (lattice spacing increases to hundreds times of the radius), the thermal accumulation effects are weak and can be neglected safely. The polarization-dependent distribution of the temperature increase of nanoparticles is observed only in the compact nanoparticle ensemble, while for a dilute ensemble, such a polarization-dependent temperature increase distribution can no longer be observed. This work may help with the understanding of the light-induced thermal transport in the 2D particle ensemble.

DOI: 10.1103/PhysRevB.105.235431

I. INTRODUCTION

Nanoscale temperature control in complex plasmonic nanoparticle ensembles has attracted a lot of interest in the fields of physics [1–4], chemistry [5–8], and biology [9–11], to name a few, in which light illumination is an efficient and common ingredient. Such a light-assisted temperature control approach has many applications, ranging from hyperthermia therapy to additive manufacturing. Nanoparticles inside the ensemble often obtain energy from the incident light and then work as heat sources heating each other. Hence, the photothermal behavior of a nanoparticle ensemble is an optical-thermal coupling process and should be analyzed from both the optical (light absorption and scattering) and thermal (heat dissipation) sides.

To understand the light-induced thermal behavior of nanoparticle ensembles well, we should investigate the optical properties of the nanoparticle ensembles first. Multiple scattering (MS) in nanoparticle ensembles will inevitably affect light absorption and, finally, will affect light-induced thermal behavior, which is named the multiple scattering effect. The coupled dipole method (CDM) is a well-known tool used for the investigation of the properties of small particles [12,13]. In the CDM, the effect of mutual multiple scattering in the nanoparticle ensemble on light absorption is considered using the external electric field experienced by each nanoparticle rather than the direct incident field (i.e., illumination field). When nanoparticles are far enough away from each other, they can be treated as optically independent. That is, the external electric field experienced by nanoparticles can directly be approximated to the incident field. Some other methods (e.g., the finite-element method [14] and the finite-difference time domain method [15], the generalized multiparticle Mie method [16,17], and the boundary element method [18–20], to name a few) can also be applied to investigate the optical properties of nanoparticle ensembles.

Then, with the aforementioned methods in hand, the optical properties of nanoparticle ensembles have been investigated widely and have been reviewed in the literature [21–23]. Collective lattice resonance for disordered and quasirandom ensembles [24] and ordered arrays [25–29] of nanoparticles have been analyzed. The effect of the array structure on the plasmonic resonance wavelength was analyzed theoretically for silver nanoparticle ensembles [30], for which extinction

*jmzhao@hit.edu.cn
†mauro.antezza@umontpellier.fr

TABLE I. Different configurations in the literature in the field of the thermal behavior of a nanoparticle (NP) ensemble under illumination.

Year	Authors	Configurations
2006	Govorov *et al.* [44]	One NP, two NPs, 2D 4 × 4 square-lattice NP ensembles
2009	Richardson *et al.* [39]	Metal NP solution
2010	Baffou *et al.* [36]	2D square-lattice NP ensembles
2013	Baffou *et al.* [40]	One-dimensional linear NP chain, 2D square-lattice NP ensembles
2018	Siahpoush *et al.* [43]	3D random NP ensembles
2019	Moularas *et al.* [42]	Core-shell NP ensembles

spectra shift was reported. Evlyukhin *et al.* [31] and Zundel and Manjavacas [32] systematically analyzed the finite-size effect on the optical response for periodic arrays of nanostructures (e.g., nanoparticles and graphene nanodisks). In addition to the above theoretical predictions, electromagnetic interactions in plasmonic nanoparticle ensembles were investigated, and the spectral shift was demonstrated experimentally [33]. The aforementioned investigations of the optical response of nanoparticle ensembles provide fundamental knowledge from the optical side to understand the photothermal behavior of nanoparticle ensembles.

From the thermal side, light absorption by each nanoparticle in the ensemble will heat the whole nanoparticle ensemble cumulatively, namely, the accumulative (collective) heating effect, which was predicted theoretically [34–38] and demonstrated experimentally [39–42]. For a small particle (the point dipole approximation is valid), a Green's function approach combining the coupled dipole method with the thermal Green's function for light-induced thermal behavior modeling of nanoparticle ensembles was proposed by Baffou *et al.* [36], in which the steady-state temperature distribution throughout arbitrary complex plasmonic systems can be calculated easily.

By means of the Green's function approach, the effect of plasmonic (optical) coupling on the photothermal behavior of an ensemble with a three-dimensional (3D) random distribution of nanoparticles was analyzed by Siahpoush *et al.* [43]. They found that the multiple scattering can reduce the temperature increase of nanoparticles compared to the case without multiple scattering at the plasmonic resonance wavelength of a single nanoparticle. Due to the thermal accumulation (TA) effect, when calculating the temperature increase of an arbitrary nanoparticle from a nanoparticle ensemble, we often cannot simply treat the nanoparticle individually, as if the rest of the nanoparticles do not exist [40,44]. Although the multiple scattering and thermal accumulation effects on the photothermal behavior of nanoparticle ensembles with different configurations have already been investigated (as summarized in Table I), no clear and quantitative regime borders of these two effects have been reported yet. A method to figure out the regime of these two effects will greatly facilitate the investigation of the photothermal behavior of nanoparticle ensembles, which is the motivation of this work.

It should be noted that, due to the multiple scattering, the light may attenuate along its propagation direction in the 3D random nanoparticle ensemble, which can also reduce the temperature increase of nanoparticles. It is hard to tell the effect of light attenuation on the temperature increase from the multiple scattering effect on inhibition of the temperature. In this work, to have a clear understanding of the multiple scattering effect on photothermal behavior without any interference from the light attenuation, we consider two-dimensional nanoparticle ensembles, for which the extension direction is perpendicular to the light propagation direction. In addition, light absorption of the nanoparticle ensemble is polarization dependent [14,22,45]. The effect of light polarization on the photothermal behavior of an ensemble composed of only a few or tens of nanoparticles has been analyzed already [14,20,46,47]. As the number of nanoparticles in the ensemble increases, the mutual interaction between nanoparticles in the ensemble becomes more and more complex, and it has remained unclear if the light polarization effect on the photothermal behavior still exists.

We address the aforementioned missing points in this paper, investigating the photothermal behavior of two-dimensional nanoparticle ensembles using the Green's function approach [36]. This work is organized as follows. In Sec. II, the coupled dipole method for light scattering and the thermal Green's function method for steady temperature spatial distribution are presented briefly, considering the mutual multiple scattering interaction and thermal accumulation effect. In addition, the physical model of the two-dimensional (2D) nanoparticle ensemble considered in this work is also given. In Sec. III, a method to clearly and quantitatively figure out the regime borders of both the multiple scattering and the thermal accumulation will be proposed as the focus of this work. Effects of both the multiple scattering and the thermal accumulation on photothermal behavior, as well as the relation between the two effects, will be discussed.

II. THEORETICAL MODELS

In this section, we describe the physical system and the theoretical models: (1) the coupled dipole method describing the light scattering and absorption of nanoparticle ensembles and (2) the thermal Green's function method describing the steady temperature spatial distribution for the nanoparticle ensembles. The SI unit system is used.

A. Physical systems: 2D nanoparticle ensembles

We investigate the thermal behavior of the 2D nanoparticle ensemble ($N \times N$ square-lattice ensemble) illuminated by an incident light, as shown in Fig. 1. The size of the nanoparticle is supposed to be small compared to the wavelength of the incident light, which results in the validity of the point dipole approximation of the nanoparticle. The incident light wave vector is against the positive z-axis direction, and the polarization direction is parallel to the x axis. The ensemble is parallel to the xoy plane. The lattice spacing is L. The nanoparticle radius is a. When analyzing the relation between the multiple scattering and collective effects on the light-induced thermal

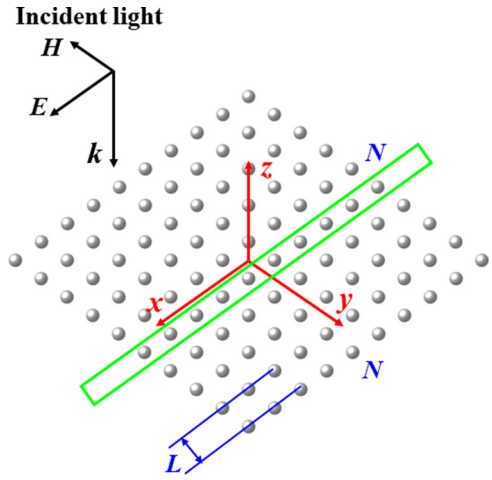

FIG. 1. Structure diagram of the two-dimensional $N \times N$ square-lattice nanoparticle ensemble. The light-induced thermal behavior of the ensemble is investigated. The lattice spacing is L. The nanoparticle radius is a. A chain of nanoparticles near the x axis is extracted out of the 2D square-lattice nanoparticle ensemble in the green frame and is defined by $y = L/2$ and $z = 0$.

behavior of the ensemble, a chain of nanoparticles of interest near the x axis is extracted out of the 2D square-lattice nanoparticle ensemble in the green frame in Fig. 1 and is defined by $y = L/2$ and $z = 0$. When analyzing the thermal accumulation effect, the nanoparticle in the first sector closest to the origin is assigned to be the central nanoparticle of the ensemble. The central nanoparticle position is defined as $x = y = L/2$.

B. Coupled dipole method

When the dipolar nanoparticle ensemble is illuminated by an incident light characterized by the electric field amplitude $\mathbf{E}^{\text{inc}}(\mathbf{r})$, the multiple scattering between each nanoparticle results in an external field $\mathbf{E}^{\text{ext}}(\mathbf{r})$ experienced by each nanoparticle, which is quite different from the incident one and yields [13,32]

$$\mathbf{E}^{\text{ext}}(\mathbf{r}_\text{i}) = \mathbf{E}^{\text{inc}}(\mathbf{r}_\text{i}) + \frac{k^2}{\epsilon_0 \epsilon_\text{m}} \sum_{\text{j}\neq\text{i}}^{N_\text{t}} \mathbf{G}(\mathbf{r}_\text{i}, \mathbf{r}_\text{j}) \cdot \mathbf{p}_\text{j}, \tag{1}$$

where $k = \sqrt{\epsilon_\text{m}}\omega/c$ is the wave vector in the host medium, ϵ_m is the host medium relative permittivity, ϵ_0 is vacuum permittivity, $N_\text{t} = N \times N$ is the total number of nanoparticles in the 2D square-lattice nanoparticle ensemble, $G(\mathbf{r}_\text{i}, \mathbf{r}_\text{j}) = \frac{e^{ikr}}{4\pi r}[(1 + \frac{ikr-1}{k^2r^2})\mathbb{I}_3 + \frac{3-3ikr-k^2r^2}{k^2r^2}\hat{\mathbf{r}} \otimes \hat{\mathbf{r}}]$ is the electric Green's function connecting two nanoparticles at $\mathbf{r}_\text{i}$ and $\mathbf{r}_\text{j}$, r is the magnitude of the separation vector $\mathbf{r} = \mathbf{r}_\text{i} - \mathbf{r}_\text{j}$, $\hat{\mathbf{r}}$ is the unit vector $\mathbf{r}/r$, $\mathbb{I}_3$ is the 3×3 identity matrix, and $\mathbf{p}_\text{j}$ is the dipole moment located at $\mathbf{r}_\text{j}$, which yields

$$\mathbf{p}_\text{j} = \epsilon_0 \epsilon_\text{m} \alpha_\text{j} \mathbf{E}^{\text{ext}}(\mathbf{r}_\text{j}), \tag{2}$$

where α_j is the polarizability of the jth particle considering the radiation correction defined as

$$\alpha_\text{j} = \left(\frac{1}{\alpha_\text{j}^0} - \frac{ik^3}{6\pi} \right)^{-1}, \tag{3}$$

where α_j^0 is the Clausius-Mossotti polarizability defined as [23,48]

$$\alpha_\text{j}^0 = 4\pi a^3 \frac{\epsilon(\omega) - \epsilon_\text{m}}{\epsilon(\omega) + 2\epsilon_\text{m}}, \tag{4}$$

where a is the nanoparticle radius. $\epsilon(\omega)$ is the relative permittivity of the nanoparticle. Then, the external field experienced by all nanoparticles in the ensemble can be rearranged in a compact and explicit way as follows:

$$\begin{pmatrix} \mathbf{E}^{\text{ext}}(\mathbf{r}_1) \\ \mathbf{E}^{\text{ext}}(\mathbf{r}_2) \\ \vdots \\ \mathbf{E}^{\text{ext}}(\mathbf{r}_{\text{N}_\text{t}}) \end{pmatrix} = \mathbb{A}^{-1} \begin{pmatrix} \mathbf{E}^{\text{inc}}(\mathbf{r}_1) \\ \mathbf{E}^{\text{inc}}(\mathbf{r}_2) \\ \vdots \\ \mathbf{E}^{\text{inc}}(\mathbf{r}_{\text{N}_\text{t}}) \end{pmatrix}, \tag{5}$$

where the $3N \times 3N$ matrix is defined as

$$\mathbb{A} = \mathbb{I}_{3N} - k^2 \begin{pmatrix} 0 & \alpha_2 \mathbf{G}_{12} & \cdots & \alpha_N \mathbf{G}_{1N} \\ \alpha_1 \mathbf{G}_{21} & 0 & \ddots & \vdots \\ \vdots & \vdots & \ddots & \alpha_N \mathbf{G}_{(N-1)N} \\ \alpha_1 \mathbf{G}_{N1} & \cdots & \alpha_{N-1} \mathbf{G}_{N(N-1)} & 0 \end{pmatrix}, \tag{6}$$

where $\mathbf{G}_{\text{ij}} = \mathbf{G}(\mathbf{r}_\text{i}, \mathbf{r}_\text{j})$ and $\mathbb{I}_{3N}$ is the $3N \times 3N$ identity matrix.

C. Thermal Green's function method

In the following, it is supposed that the thermal conductivity of the nanoparticle is much higher than that of the host medium. Under such an approximation, the temperature can be considered uniform inside the nanoparticle [36]. For the considered metal Ag nanoparticle ensembles embedded in water, the thermal conductivity of the metal particle (Ag, $\kappa_{\text{particle}} = 429\ \text{W m}^{-1}\ \text{K}^{-1}$) is much higher than that of the host medium (water, $\kappa = 0.6\ \text{W m}^{-1}\ \text{K}^{-1}$). The temperature increase ΔT_i (relative to the ambient temperature) inside the ith nanoparticle of the ensemble induced by the incident light yields [36]

$$\Delta T_\text{i} = \sum_{j=1}^{N_\text{t}} G_\text{t}(\mathbf{r}_\text{i}, \mathbf{r}_\text{j}) Q_\text{j}, \tag{7}$$

where $Q_\text{j} = \frac{1}{2}\sigma_{\text{abs}} n c \epsilon_0 |\mathbf{E}^{\text{ext}}(\mathbf{r}_\text{j})|^2$, $\sigma_{\text{abs}} = k\text{Im}(\alpha_\text{j}) - \frac{\text{k}^4}{6\pi}|\alpha_\text{j}|^2$ is the absorption cross section of the jth nanoparticle, and $n = \sqrt{\epsilon_\text{m}}$ is the refractive index of the host medium. The thermal Green's function $G_\text{t}(\mathbf{r}_\text{i}, \mathbf{r}_\text{j})$ with $\mathbf{r}_\text{i}$ different from $\mathbf{r}_\text{j}$ is a scalar Green's function $G(\mathbf{r}, \mathbf{r}_\text{j})$ at $\mathbf{r}_\text{i}$, which is associated with the following Poisson equation with a Dirac source distribution

$\delta(\mathbf{r}-\mathbf{r}_j)$ in an infinite isotropic medium:

$$\nabla\cdot[-\kappa\nabla T(\mathbf{r})]=\sum_{j=1}^{N_t}Q_j\delta(\mathbf{r}-\mathbf{r}_j). \tag{8}$$

The scalar Green's function $G(\mathbf{r},\mathbf{r}_j)$ is

$$G(\mathbf{r},\mathbf{r}_j)=\frac{1}{4\pi\kappa|\mathbf{r}-\mathbf{r}_j|}, \tag{9}$$

where κ is the thermal conductivity of the host medium. Hence, for $\mathbf{r}_i$ different from $\mathbf{r}_j$, $G_t(\mathbf{r}_i,\mathbf{r}_j)=1/(4\pi\kappa|\mathbf{r}_i-\mathbf{r}_j|)$, and for $\mathbf{r}_i$ equal to $\mathbf{r}_j$, $G_t(\mathbf{r}_i,\mathbf{r}_i)=1/(4\pi\kappa a)$ [36].

It is worth mentioning that the thermal emission of the particles may also affect the temperature increase ΔT_i. For a nonabsorbing host medium, the net emitted power from particle j to the thermal bath can be defined as $\mathcal{P}_{j\leftrightarrow B}=\hat{\sigma}_{abs}n^2\sigma_B(T_j^4-T_{env}^4)$ [49,50], where $\hat{\sigma}_{abs}$ is the averaged thermal absorption cross section, $n=\sqrt{\epsilon_m}$ is the refractive index, σ_B is the Stefan-Boltzmann constant, T_{env} is the environment temperature, and T_j is the temperature of particle j. For the considered geometry where the power absorbed from the incident light is much more significant than the power exchanged with the environment, $\mathcal{P}_{j\leftrightarrow B}$ can be neglected with respect to Q_j in Eq. (7).

Another important factor that may significantly influence the temperature increase of nanoparticles is the thermal boundary resistance around the particles (e.g., the internal thermal resistance, the interfacial thermal resistance, and the one caused by the molecular coating) [51–54], which is well acknowledged to play a key role in nanoparticle-based experiments influencing the heat transfer between the inner plasmonic nanoparticle and the outer surrounding host medium [55]. For the thermal boundary resistance (TBR) caused by the molecular coating, it has been demonstrated that this kind of TBR indeed can affect the temperature inside the nanoparticle; however, such TBR would not change the temperature distribution in the host medium [36]. In addition, in Ref. [51], the authors demonstrated that the internal thermal resistance for the silver nanoparticle embedded in the water is negligible. As for the interfacial thermal resistance, we analyzed its effect on the temperature by applying the spherical heat transfer model and found that this kind of TBR has an effect on the temperature similar to that of the molecular coating, which will be discussed in the Appendix in detail.

Although different kinds of TBRs can exist at the water-silver nanoparticle interface, all of these kinds of TBRs will bring a jump in the temperature only inside the nanoparticles and will not change the temperature outside the nanoparticles, which is what usually matters when studying light-induced phenomena. The temperature outside nanoparticles is dependent on only the power Q released by the nanoparticle absorbed from the incident light and the thermal conductivity of the surrounding medium. That is to say, the temperature in the surrounding medium is dependent only on the multiple scattering and the thermal accumulation and will not change regardless of whether there are TBRs or not. To analyze the relation of the multiple scattering and the thermal accumulation with the temperature in the surrounding medium, we use a simple case that neglects the TBRs, which will not change the main conclusions in this work concerning the multiple scattering and thermal accumulation.

III. RESULTS AND DISCUSSION

The photothermal behavior of two-dimensional nanoparticle ensembles is analyzed with particular focus on the multiple scattering and thermal accumulation effects. Nanoparticle radius a is 5 nm (with a diameter of 10 nm). Nanoparticles are composed of metal Ag. The bulk dielectric function of Ag given in Ref. [56] is used in this work; it has been experimentally demonstrated to be valid for the Ag nanoparticle of the diameter down to at least 7 nm [57]. It is worth mentioning that it is easy to include the confinement effect in the present theory only by changing the nanoparticle permittivity. The incident light wavelength is fixed at 383 nm, which corresponds to the plasmonic resonance of a Ag nanoparticle embedded in water with a relative permittivity of $\epsilon_m=1.77$ and thermal conductivity of $\kappa=0.6\,\mathrm{W\,m^{-1}\,K^{-1}}$. Although we focus on only the multiple scattering effect at resonance frequency in this work, it is noted that the effect of multiple scattering on the photothermal behavior is wavelength dependent. We discuss the multiple scattering effect on photothermal behavior by considering only water as a host medium in this work. As indicated by our previous work [58], the relative permittivity of the host medium significantly affects the nanoparticle polarizability, which is strongly relevant to the temperature increase of nanoparticles determined by Eq. (7) combined with $\sigma_{abs}=k\mathrm{Im}(\alpha_j)-\frac{k^4}{6\pi}|\alpha_j|^2$ and $Q_j=\frac{1}{2}\sigma_{abs}nc\epsilon_0|\mathbf{E}^{ext}(\mathbf{r}_j)|^2$. Thus, by tailoring the host medium relative permittivity, one may consequently control the photothermal behavior of nanoparticles. The incident light intensity I_0 is 0.5 mW $\mu\mathrm{m}^{-2}$. The lattice spacing L is at least 3 times larger than the particle radius, which makes the dipole approximation valid [59–61]. The dimensionless parameters X and Y are defined as $x/[L(N-1)]$ and $y/[L(N-1)]$, respectively.

A. Relation between the multiple scattering and thermal accumulation effects

The light-induced thermal behavior of the nanoparticle ensemble is affected by two main factors, i.e., (1) the multiple scattering effect [43] and (2) the thermal accumulation effect [2,36]. We clarify the two factors briefly first and then discuss the relation between them.

Multiple scattering effect. The multiple scattering effect concerns the light scattering and absorption of the nanoparticles. As mentioned in Sec. II B, the external field $\mathbf{E}^{ext}(\mathbf{r}_i)$ experienced by the ith nanoparticle at $\mathbf{r}_i$ can be obtained by Eq. (1), where the second term on the right side corresponds to the multiple scattering. When the multiple scattering is negligible, the external field $\mathbf{E}^{ext}(\mathbf{r}_i)$ is directly equal to the illuminating incident field $\mathbf{E}^{inc}(\mathbf{r}_i)$ after neglecting the second term on the right side in Eq. (1).

Thermal accumulation effect. The thermal accumulation effect concerns the thermal diffusion process in the nanoparticle ensemble. As mentioned in Sec. II C, the temperature increase ΔT experienced by the ith nanoparticle calculated by Eq. (7) has two contributions: (1) its own heat generation ΔT_S and

(2) the heat generated by the other $N_t - 1$ nanoparticles ΔT^{ext} under illumination in the ensemble, which yield

$$\Delta T = \Delta T_S + \Delta T^{ext}, \tag{10}$$

where $\Delta T_S = G_t(\mathbf{r}_i, \mathbf{r}_i)Q_i$ is the temperature increase of the ith nanoparticle due to its own heat generation and $\Delta T^{ext} = \sum_{j\neq i} G_t(\mathbf{r}_i, \mathbf{r}_j)Q_j$ is the temperature increase of the ith nanoparticle due to the heat generated by the other $N_t - 1$ nanoparticles.

The thermal accumulation effect corresponds to the second term on the right side of Eq. (10). When the thermal accumulation effect is negligible, the second term on the right side of Eq. (10) is negligible. Each nanoparticle in the nanoparticle ensemble can be treated as an isolated hot spot.

To quantitatively analyze the multiple scattering and the thermal accumulation effect, the parameter φ is defined as follows:

$$\varphi = \Delta T/\Delta T_{\nu=0 \text{ or } S}, \tag{11}$$

where $\Delta T_{\nu=0 \text{ or } S}$ correspond to the temperature increase without the multiple scattering effect and the temperature increase due to only its own heat generation, respectively. We show the dependence of φ for both the multiple scattering effect and thermal accumulation effect on two parameters: (1) the dimensionless lattice spacing L/a and (2) the dimensionless X in Fig. 2. We consider 14×14 square-lattice nanoparticle ensembles. The blue dashed line corresponding to the dimensionless parameter defined in Ref. [2], $\zeta = L/(3aN) = 1$, is added for reference. $\zeta \gg 1$ indicates a negligible thermal accumulation effect. $\zeta \ll 1$ indicates a strong thermal accumulation effect.

As shown in Fig. 2(a), regions with three different $\varphi = \Delta T/\Delta T_0$ can be clarified: $\varphi < 1$, $\varphi \approx 1$, and $\varphi > 1$, respectively. The multiple scattering significantly inhibits ΔT in the region where $\varphi = \Delta T/\Delta T_0 < 1$, where the lattice spacing is relatively short and the nanoparticle ensemble is relatively dense. The multiple scattering enhances ΔT in the region $\varphi = \Delta T/\Delta T_0 > 1$. We can see that the enhancement region is right around the blue line. The multiple scattering effect is negligible for most of the region, where $\varphi = \Delta T/\Delta T_0 \approx 1$. We also observe that there are some separate regions where the multiple scattering inhibits ΔT embedded in the region where the multiple scattering is negligible. In a previous study, the 3D random distribution was considered [43]. The authors reported that the multiple scattering in the nanoparticle ensembles can significantly inhibit the photothermal behavior without revealing the condition when such multiple scattering is negligible from the nanoparticle ensemble structure point of view. As shown in Fig. 2(a), when the parameter φ approaches 1, the multiple scattering starts to become less important. When the lattice space L becomes comparable to or even larger than tens of a, then multiple scattering inside the nanoparticle ensembles consequently becomes negligible.

As shown in Fig. 2(b), $\varphi = \Delta T/\Delta T_S \geqslant 1$ for the whole region. The region $\varphi = \Delta T/\Delta T_S \approx 1$ is the region where the thermal accumulation effect is negligible. The negligible thermal accumulation effect region is consistent with the region $\zeta \gg 1$. For the strong thermal accumulation effect region ($\zeta \ll 1$), we can see $\varphi \gg 1$; the thermal accumulation effect is strongly in favor of ΔT. It is noted that the condition

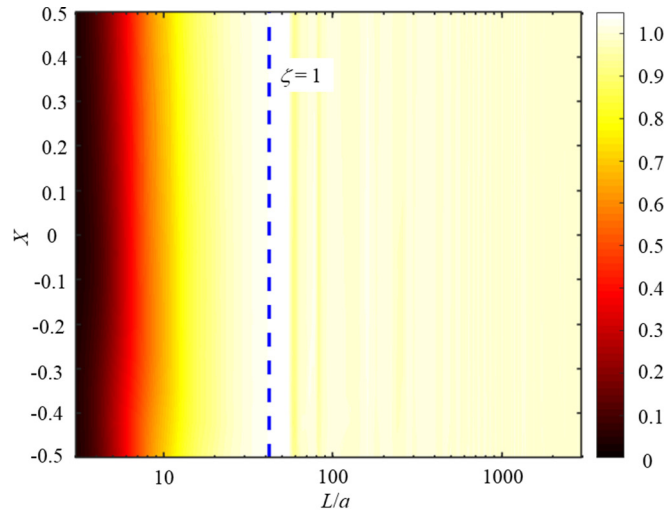

(a) Multiple scattering effect

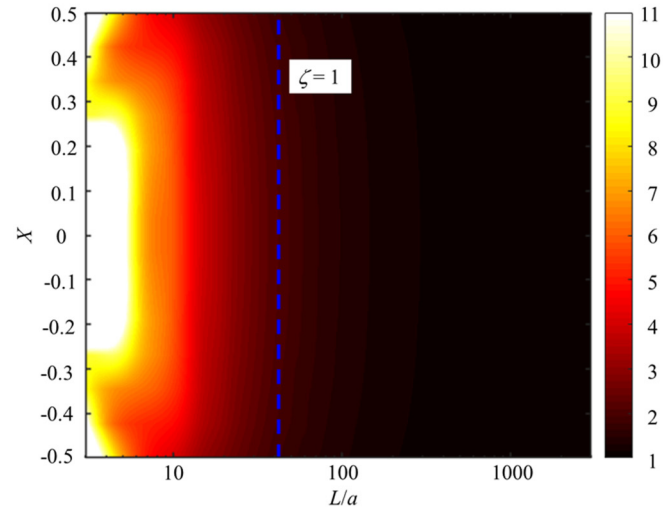

(b) Thermal accumulation effect

FIG. 2. Dependence of the parameter φ on the lattice spacing and dimensionless X. (a) We define a parameter $\varphi = \Delta T/\Delta T_S$ to evaluate the thermal accumulation effect. ΔT_S is the temperature increase induced by its own heat generation. (b) We define a parameter $\varphi = \Delta T/\Delta T_0$ to evaluate the multiple scattering effect. ΔT_0 is the temperature increase without the multiple scattering effect. The nanoparticle number is $N = 14$ for each lateral edge. The blue dashed line corresponding to the dimensionless parameter defined in Ref. [2], $\zeta = L/(3aN) = 1$, is added for reference.

$\zeta \gg 1$ for the region with a negligible thermal accumulation effect defined in Ref. [2] is not an explicit regime border description. However, the condition that the dimensionless parameter $\varphi \approx 1$ clearly determines the regime border of the thermal accumulation explicitly, where the lattice spacing is around $600a$. When the lattice spacing increases to $600a$, then each nanoparticle in the ensemble works as a hot spot separately, without any influence from nearby nanoparticles, and the thermal accumulation effect consequently becomes negligible.

The multiple scattering effect can compete with the thermal accumulation effect for dense nanoparticle ensembles and can also cooperate with the thermal accumulation effect to

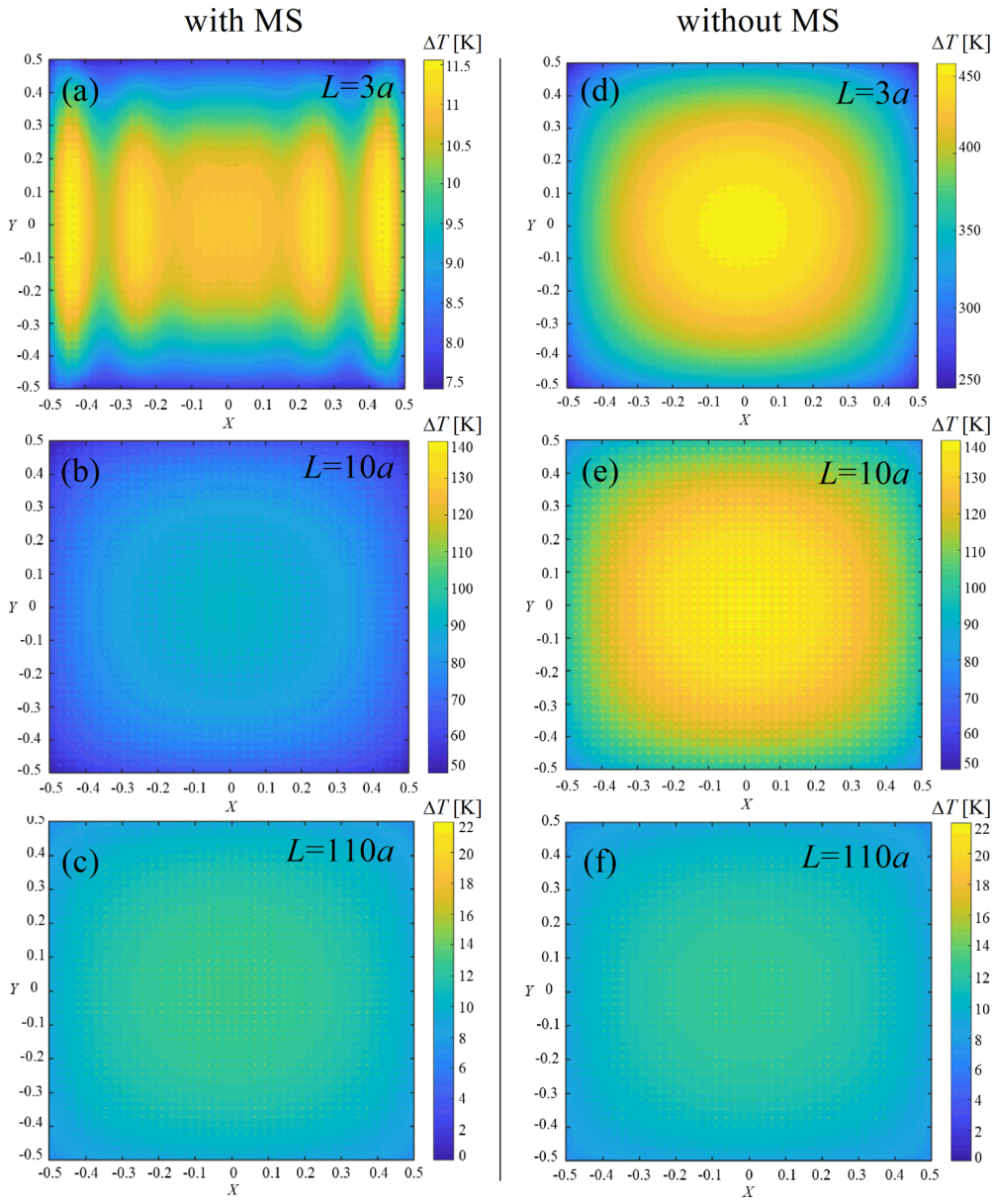

FIG. 3. The temperature increase distribution for a 2D ensemble with several different lattice spacings ($L = 3a$, $10a$, and $110a$): (a)–(c) ΔT with the multiple scattering effect and (d)-(f) ΔT without the multiple scattering effect. The number of nanoparticles for each lateral edge $N = 40$. The dimensionless parameters are $X = x/[L(N-1)]$ and $Y = y/[L(N-1)]$.

enhance ΔT. For loose enough ensembles, both the multiple scattering effect and the thermal accumulation effect are negligible, and the plasmonic nanoparticle can safely be treated as an isolated hot spot.

B. Multiple scattering effect on photothermal behavior

In this section, the optical plasmonic coupling effects on the photothermal behavior of the 2D finite-size square-lattice nanoparticle ensemble are analyzed. It is worth mentioning that the optical plasmonic coupling inhibits the temperature increase of the 3D randomly distributed nanoparticle ensemble [43].

The temperature increase distribution for the 2D ensemble with several different lattice spacings is shown in Fig. 3 ($L = 3a$, $10a$, and $110a$, respectively): Figs. 3(a)–3(c) show the temperature increase distribution with the multiple scattering effect, and Figs. 3(d)–3(f) show the temperature increase distribution without the multiple scattering effect. The nanoparticle number for each lateral edge $N = 40$.

For dense ensembles ($L = 3a$ and $10a$), the temperature increase with multiple scattering shown in Figs. 3(a) and 3(b) is much less than that without the multiple scattering shown in Figs. 3(d) and 3(e), respectively. For the dilute ensemble ($L = 110a$), the temperature increase distribution with multiple scattering shown in Fig. 3(c) is nearly the same as that without the multiple scattering shown in Fig. 3(f). The strong multiple scattering significantly inhibits the temperature increase of the nanoparticles in the 2D square-lattice ensemble. When the lattice spacing increases, the multiple scattering significantly decreases, which accounts for the negligible inhibition of ΔT.

We extract a chain of nanoparticles of interest near the x axis out of the 2D square-lattice nanoparticle ensemble,

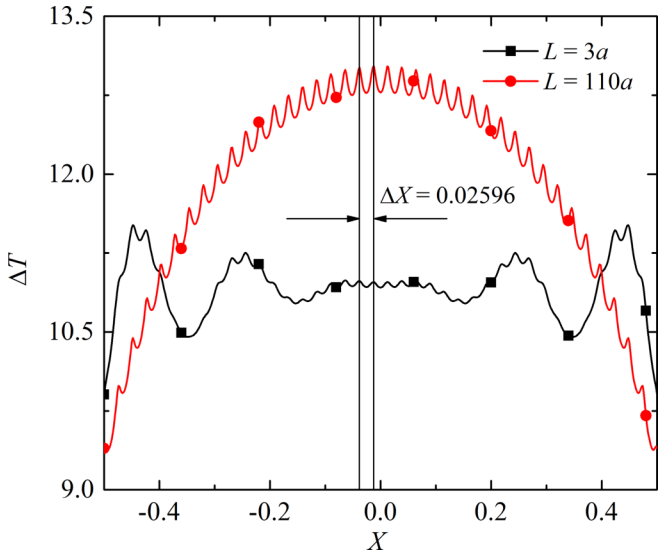

FIG. 4. Temperature increase along the chain of interest with two different lattice spacings ($L = 3a$ and $110a$). The separation distance between the neighboring peaks $\Delta X \approx 0.02596$ for the two considered ensembles, which corresponds to $\Delta x \approx L$.

as shown in Fig. 1. The chain is defined by $y = L/2$ and $z = 0$. The temperature increase along the nanoparticle chain of interest with two different lattice spacings ($L = 3a$ and $110a$) is shown in Fig. 4. The dimensionless and real separation distances between the neighboring peaks shown in Fig. 4 are $\Delta X \approx 0.02596$ and $\Delta x \approx L$ for the two considered ensembles with two different lattice spacings ($L = 3a$ and $110a$), respectively, which is consistent with the reported results [40]. For the dense ensemble ($L = 3a$), we can observe another obvious oscillation of the temperature increase near the boundary along the x axis, as shown in Figs. 3(a) and 4. For the dilute ensemble ($L = 110a$), the temperature increase ΔT decreases monotonically in general from the center to the boundary along the x axis. The strong multiple scattering in the dense ensemble accounts for the oscillation of the temperature increase ΔT from the center to the boundary of the ensemble along the x axis.

As shown in Figs. 3(a)–3(c), the temperature increase for the dense ensemble ($L = 3a$) is angle dependent (seen from the ensemble center), which is quite different from the angle-independent temperature increase for dilute ensembles ($L = 10a$ and $110a$). For the dilute nanoparticle ensembles, the multiple scattering becomes less important, and thus, each particle works as a separate heat source for the temperature increase, which results in the angle-independent temperature distribution. The multiple scattering in the dense particle ensemble is expected to be strong and polarization dependent, which may account for the angle-dependent temperature distribution. Hence, to some extent, we can tailor the temperature increase distribution using light polarization. However, it is worth mentioning that the light-induced heat transfer behavior in the nanostructures (e.g., dense particle ensembles) is not always polarization dependent. Recently, polarization-independent isosbestic temperature increase behavior of nanostructures was proposed [45,47].

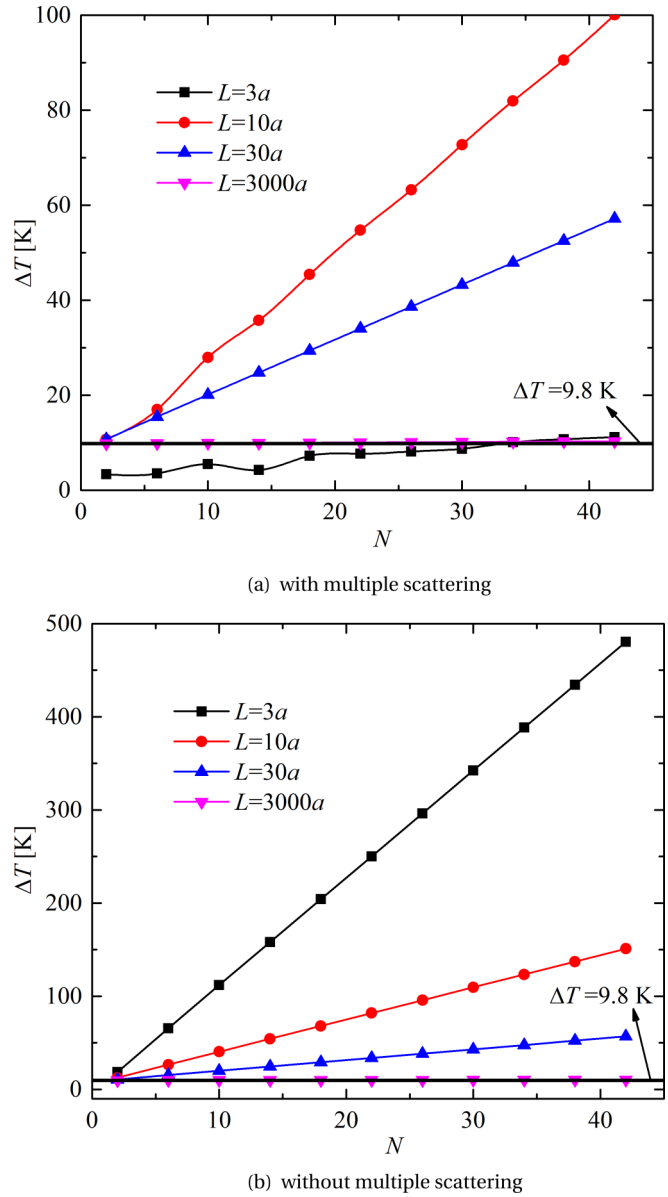

FIG. 5. Dependence of ΔT of the ensemble center on the nanoparticle number N in each lateral edge: (a) with the multiple scattering effect and (b) without the multiple scattering effect. Lattice spacing $L = 3a$, $10a$, $30a$, and $3000a$. Metal Ag is used. The temperature increase $\Delta T = 9.8$ K for the isolated single nanoparticle is also added for reference.

C. Thermal accumulation effect

The dependence of ΔT of the center of the 2D square-lattice ensemble on the nanoparticle number N in each lateral edge is shown in Fig. 5 with the multiple scattering effect [Fig. 5(a)] and without the multiple scattering effect [Fig. 5(c). Four different lattice spacings are considered, $L = 3a$, $10a$, $30a$, and $3000a$. The temperature increase $\Delta T = 9.8$ K for the isolated single nanoparticle is also added for reference.

For the compact ensembles ($L = 3a$ and $10a$), ΔT increases nonlinearly with N. However, for the loose ensemble ($L = 30a$), the linear dependence of ΔT on N can be observed, which is consistent with the results reported in

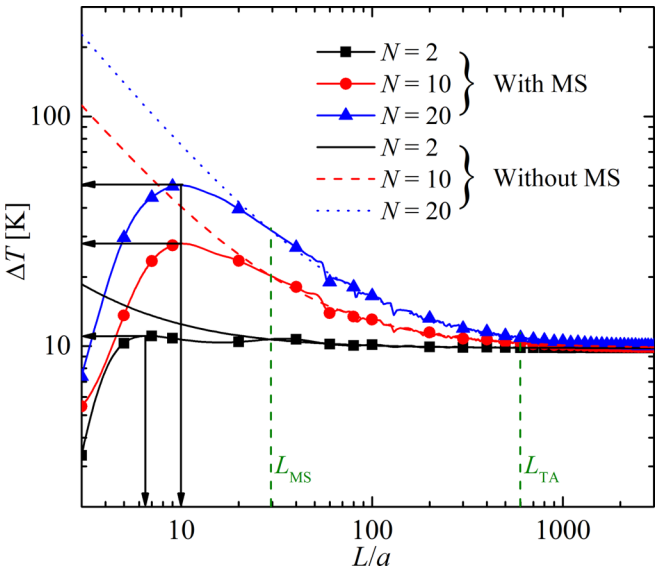

FIG. 6. Dependence of ΔT for the ensemble center on the lattice spacing L/a. $N = 2$, 10, and 20. ΔT both with and without multiple scattering effects are considered. From $L = L_{\mathrm{MS}}$, ΔT with and without multiple scattering effect start to become identical. From $L = L_{\mathrm{TA}}$, ΔT for ensembles composed of different numbers of nanoparticles start to become identical.

Ref. [36]. For the compact ensemble (e.g., $L = 3a$), the temperature increase ΔT for the central nanoparticle is even less than that of the isolated single nanoparticle. For all the considered ensembles with different lattice spacings, the temperature increase ΔT without the multiple scattering effect increases linearly with N, as shown in Fig. 5(b). The strong multiple scattering for the compact ensembles accounts for the nonlinear dependence of ΔT on N, as observed in Fig. 5(a). For the extremely loose ensemble ($L = 3000a$), the multiple scattering and thermal accumulation effects are negligible, which accounts for the temperature increase ΔT for the central nanoparticle being the same as that of the isolated single nanoparticle.

From Figs. 5(a) and 5(b), in general, for an ensemble composed of a certain number of nanoparticles, ΔT without the multiple scattering effect increases monotonically with the lattice spacing, while ΔT with the multiple scattering effect increases at first and then decreases with the lattice spacing. The dependence of ΔT for the ensemble center on the lattice spacing L/a is shown in Fig. 6. Ensembles of three different sizes are considered, $N = 2$, 10, and 20. ΔT both with and without multiple scattering effects are considered. From $L = L_{\mathrm{MS}}$ (the multiple scattering length scale), ΔT with and without the multiple scattering effect start to become identical, where the multiple scattering is negligible. From $L = L_{\mathrm{TA}}$ (the thermal accumulation length scale), ΔT for ensembles composed of different amounts of nanoparticles start to become identical, where the thermal accumulation effect is negligible. The length L_{TA} where the thermal accumulation effect is negligible is much larger than the length L_{MS} where multiple scattering starts to be less important. When the thermal accumulation effect is negligible, the multiple scattering also cannot be observed. However, when the multiple scattering effect is negligible, the thermal accumulation effect on the photothermal behavior can exist if the lattice spacing L is not large enough.

When considering the case with no multiple scattering effect, the temperature increase ΔT for the central nanoparticle decreases monotonically with L/a. The pure thermal accumulation effect accounts for the monotonic dependence of ΔT on L/a. When considering the cases with the multiple scattering effect, ΔT increases at first and then decreases with L/a, as shown with the lines with symbols in Fig. 6. The thermal accumulation effect together with the multiple scattering effect accounts for the nonmonotonic dependence of ΔT on L/a.

We can also notice that small oscillations of ΔT occur at around few tens of L/a in Fig. 6. Note that $a = 5$ nm, so the lattice spacings L corresponding to small oscillations are comparable to or even larger than the considered wavelength (383 nm). According to Zou and Schatz [62], for a fixed wavelength, the extinction efficiency of two-dimensional hexagonal arrays is not monotonously dependent on the lattice spacing, as shown in Fig. 3 of Ref. [62]. Such nonmonotonously dependent optical properties may account for the small oscillations of ΔT when increasing L/a for two-dimensional nanoparticle arrays.

IV. CONCLUSION

Light-induced heat transfer of the two-dimensional nanoparticle ensembles embedded in water was investigated by means of the Green's function approach with a focus on proposing a clear regime map for both the multiple scattering and the thermal accumulation. The dimensionless parameter φ was defined to quantify the multiple scattering and collective effects on photothermal behavior. For a 2D ordered nanoparticle ensemble, similar to the 3D random nanoparticle ensemble, multiple scattering can also inhibit the temperature increase ΔT of nanoparticles. The more compact the nanoparticle ensemble is, the stronger the multiple scattering effect on thermal behavior is. When the lattice spacing increases to dozens times of the radius, the multiple scattering becomes insignificant. In addition, when $\varphi \approx 1$ and lattice spacing increases to hundreds times of the radius, the thermal accumulation effects are weak and can be neglected safely. The distribution of the temperature increase of nanoparticles is polarization dependent, especially for the compact nanoparticle ensemble. However, for a dilute ensemble, such a polarization-dependent temperature increase distribution cannot be observed. The temperature increase ΔT of the center of the ensemble increases linearly with increasing the ensemble size without considering multiple scattering. However, when considering multiple scattering, for the compact ensemble, ΔT increases nonlinearly with increasing the ensemble size. For a fixed ensemble size, ΔT increases nonlinearly with increasing the lattice spacing. This work may help with the understanding of light-induced thermal transport in a 2D particle ensemble.

ACKNOWLEDGMENTS

This work is supported by the National Natural Science Foundation of China (Grant No. 51976045). M.G.L. also thanks the China Postdoctoral Science Foundation (Grant No. 2021M700991) for support. In addition, we acknowledge

greatly the kind and helpful suggestions from the two anonymous reviewers.

APPENDIX: INFLUENCE OF THE INTERFACIAL THERMAL RESISTANCE ON THE TEMPERATURE PROFILE

We applied a spherical heat transfer model to investigate the effect of the interfacial thermal resistance between a nanoparticle and water on the temperature increase. Considering that the thermal conductivity of the nanoparticle $\kappa_{\text{particle}} \gg \kappa$ (the conductivity of the surrounding medium), the temperature inside the nanoparticle ($r < a$) is uniform, T_0. The general formula for the temperature outside the nanoparticle ($r > a$) is $T(r) = C_1/r + C_2$, where the constants C_1 and C_2 can be obtained by applying the boundary conditions. The interfacial thermal resistance is R. The power absorbed by the nanoparticle with radius a from incident light is Q, which is released to the surrounding medium. We have the following boundary conditions:

$$\begin{aligned} &T(r \to \infty) = 0, \\ &\kappa\left(\frac{C_1}{r^2}\right) = \frac{Q}{4\pi r^2}. \end{aligned} \tag{A1}$$

We can find that $C_1 = \frac{Q}{4\pi\kappa}$ and $C_2 = 0$. Hence, the temperature outside the nanoparticle yields

$$T(r) = \frac{Q}{4\pi\kappa r}. \tag{A2}$$

At the interface of the nanoparticle and water, we have the following relation:

$$\frac{T_0 - T(r)|_{r\to a}}{R} = \frac{Q}{4\pi a^2}. \tag{A3}$$

Therefore, the temperature inside the nanoparticle is

$$T_0 = \frac{Q}{4\pi a} + \frac{QR}{4\pi a^2}. \tag{A4}$$

The whole temperature profile yields

$$\begin{aligned} &r < a, \quad T_0 = \frac{Q}{4\pi a} + \frac{QR}{4\pi a^2}, \\ &r \geqslant a, \quad T(r) = \frac{Q}{4\pi\kappa r}. \end{aligned} \tag{A5}$$

From Eq. (A5) for the temperature profile of the whole domain, the interfacial thermal resistance R will not change the temperature outside the nanoparticles ($r \geqslant a$), which usually matters when studying the light-induced phenomena, similar to what is observed for the coating-induced thermal resistance reported in Ref. [36]. The interfacial thermal resistance R may significantly affect the temperature inside the nanoparticles, which will bring an additional temperature increase $\frac{QR}{4\pi a^2}$ compared to the previous one by neglecting the interfacial thermal resistance. Especially, for a small particle with a large interfacial thermal resistance R, the temperature jump across the nanoparticle-water interface will be significant.

[1] G. Baffou, F. Cichos, and R. Quidant, Applications and challenges of thermoplasmonics, Nat. Mater. **19**, 946 (2020).

[2] G. Baffou, I. Bordacchini, A. Baldi, and R. Quidant, Simple experimental procedures to distinguish photothermal from hot-carrier processes in plasmonics, Light: Sci. Appl. **9**, 108 (2020).

[3] O. Blum and N. T. Shaked, Prediction of photothermal phase signatures from arbitrary plasmonic nanoparticles and experimental verification, Light: Sci. Appl. **4**, e322 (2015).

[4] S. A. Maier, M. L. Brongersma, P. G. Kik, S. Meltzer, A. A. G. Requicha, and H. A. Atwater, Plasmonics—A route to nanoscale optical devices, Adv. Mater. **13**, 1501 (2001).

[5] X. Q. Li, X. Zhang, H. O. Everitt, and J. Liu, Light-induced thermal gradients in ruthenium catalysts significantly enhance ammonia production, Nano Lett. **19**, 1706 (2019).

[6] L. Zhou, D. F. Swearer, C. Zhang, H. Robatjazi, H. Zhao, L. Henderson, L. Dong, P. Christopher, E. A. Carter, P. Nordlander, and N. J. Halas, Quantifying hot carrier and thermal contributions in plasmonic photocatalysis, Science **362**, 69 (2018).

[7] K. Saha, S. S. Agasti, C. Kim, X. Li, and V. M. Rotello, Gold nanoparticles in chemical and biological sensing, Chem. Rev. **112**, 2739 (2012).

[8] P. V. Kamat, Photophysical, photochemical and photocatalytic aspects of metal nanoparticles, J. Phys. Chem. B **106**, 7729 (2002).

[9] M. B. Cortie, D. L. Cortie, and V. Timchenko, Heat transfer from nanoparticles for targeted destruction of infectious organisms, Int. J. Hyperthermia **34**, 157 (2018).

[10] H. Šípová, L. Shao, N. Odebo Länk, D. Andrén, and M. Käll, Photothermal DNA release from laser-tweezed individual gold nanomotors driven by photon angular momentum, ACS Photonics **5**, 2168 (2018).

[11] S. Jones, D. Andrén, P. Karpinski, and M. Käll, Photothermal heating of plasmonic nanoantennas: Influence on trapped particle dynamics and colloid distribution, ACS Photonics **5**, 2878 (2018).

[12] O. Merchiers, F. Moreno, F. González, and J. M. Saiz, Light scattering by an ensemble of interacting dipolar particles with both electric and magnetic polarizabilities, Phys. Rev. A **76**, 043834 (2007).

[13] G. W. Mulholland, C. F. Bohren, and K. A. Fuller, Light scattering by agglomerates: Coupled electric and magnetic dipole method, Langmuir **10**, 2533 (1994).

[14] R. Borah and S. W. Verbruggen, Coupled plasmon modes in 2D gold nanoparticle clusters and their effect on local temperature control, J. Phys. Chem. C **123**, 30594 (2019).

[15] A. E. Ershov, V. S. Gerasimov, R. G. Bikbaev, S. P. Polyutov, and S. V. Karpov, Mode coupling in arrays of Al nanoparticles, J. Quantum Spectrosc. Radiat. Transfer **248**, 106961 (2020).

[16] Y. L. Xu and N. G. Khlebtsov, Orientation-averaged radiative properties of an arbitrary configuration of scatterers, J. Quantum Spectrosc. Radiat. Transfer **79–80**, 1121 (2003).

[17] B. Khlebtsov, V. Zharov, A. Melnikov, V. Tuchin, and N. Khlebtsov, Optical amplification of photothermal therapy with gold nanoparticles and nanoclusters, Nanotechnology **17**, 5167 (2006).

[18] F. J. García de Abajo and A. Howie, Relativistic Electron Energy Loss and Electron-Induced Photon Emission in Inhomogeneous Dielectrics, Phys. Rev. Lett. **80**, 5180 (1998).

[19] F. J. García de Abajo and A. Howie, Retarded field calculation of electron energy loss in inhomogeneous dielectrics, Phys. Rev. B **65**, 115418 (2002).

[20] G. Baffou, R. Quidant, and F. J. García de Abajo, Nanoscale control of optical heating in complex plasmonic systems, ACS Nano **4**, 709 (2010).

[21] F. J. García De Abajo, Colloquium: Light scattering by particle and hole arrays, Rev. Mod. Phys. **79**, 1267 (2007).

[22] M. B. Ross, C. A. Mirkin, and G. C. Schatz, Optical properties of one-, two-, and three-dimensional arrays of plasmonic nanostructures, J. Phys. Chem. C **120**, 816 (2016).

[23] V. G. Kravets, A. V. Kabashin, W. L. Barnes, and A. N. Grigorenko, Plasmonic surface lattice resonances: A review of properties and applications, Chem. Rev. **118**, 5912 (2018).

[24] V. I. Zakomirnyi, S. V. Karpov, H. Ågren, and I. L. Rasskazov, Collective lattice resonances in disordered and quasi-random all-dielectric metasurfaces, J. Opt. Soc. Am. B **36**, E21 (2019).

[25] A. D. Utyushev, V. I. Zakomirnyi, A. E. Ershov, V. S. Gerasimov, S. V. Karpov, and I. L. Rasskazov, Collective lattice resonances in all-dielectric nanostructures under oblique incidence, Photonics **7**, 24 (2020).

[26] A. Manjavacas, L. Zundel, and S. Sanders, Analysis of the limits of the near-field produced by nanoparticle arrays, ACS Nano **13**, 10682 (2019).

[27] V. I. Zakomirnyi, A. E. Ershov, V. S. Gerasimov, S. V. Karpov, H. Ågren, and I. L. Rasskazov, Collective lattice resonances in arrays of dielectric nanoparticles: A matter of size, Opt. Lett. **44**, 5743 (2019).

[28] M. Ramezani, G. Lozano, M. A. Verschuuren, and J. Gómez-Rivas, Modified emission of extended light emitting layers by selective coupling to collective lattice resonances, Phys. Rev. B **94**, 125406 (2016).

[29] S. Rodriguez, M. Schaafsma, A. Berrier, and J. G. Rivas, Collective resonances in plasmonic crystals: Size matters, Phys. B (Amsterdam, Neth.) **407**, 4081 (2012).

[30] L. L. Zhao, K. L. Kelly, and G. C. Schatz, The extinction spectra of silver nanoparticle arrays: Influence of array structure on plasmon resonance wavelength and width, J. Phys. Chem. B **107**, 7343 (2003).

[31] A. B. Evlyukhin, C. Reinhardt, A. Seidel, B. S. Luk'yanchuk, and B. N. Chichkov, Optical response features of Si-nanoparticle arrays, Phys. Rev. B **82**, 045404 (2010).

[32] L. Zundel and A. Manjavacas, Finite-size effects on periodic arrays of nanostructures, J. Phys. Photonics **1**, 015004 (2018).

[33] A. Bouhelier, R. Bachelot, J. S. Im, G. P. Wiederrecht, G. Lerondel, S. Kostcheev, and P. Royer, Electromagnetic interactions in plasmonic nanoparticle arrays, J. Phys. Chem. B **109**, 3195 (2005).

[34] G. Baffou and R. Quidant, Thermo-plasmonics: Using metallic nanostructures as nano-sources of heat, Laser Photonics Rev. **7**, 171 (2013).

[35] I.-W. Un and Y. Sivan, Size-dependence of the photothermal response of a single metal nanosphere, J. Appl. Phys. **126**, 173103 (2019).

[36] G. Baffou, R. Quidant, and C. Girard, Thermoplasmonics modeling: A Green's function approach, Phys. Rev. B **82**, 165424 (2010).

[37] R. Gillibert, F. Colas, M. L. de La Chapelle, and P. G. Gucciardi, Heat dissipation of metal nanoparticles in the dipole approximation, Plasmonics **15**, 1001 (2020).

[38] A. Heber, M. Selmke, and F. Cichos, Metal nanoparticle based all-optical photothermal light modulator, ACS Nano **8**, 1893 (2014).

[39] H. H. Richardson, M. T. Carlson, P. J. Tandler, P. Hernandez, and A. O. Govorov, Experimental and theoretical studies of light-to-heat conversion and collective heating effects in metal nanoparticle solutions, Nano Lett. **9**, 1139 (2009).

[40] G. Baffou, P. Berto, E. Bermúdez Ureña, R. Quidant, S. Monneret, J. Polleux, and H. Rigneault, Photoinduced heating of nanoparticle arrays, ACS Nano **7**, 6478 (2013).

[41] G. Baffou, E. B. Ureña, P. Berto, S. Monneret, R. Quidant, and H. Rigneault, Deterministic temperature shaping using plasmonic nanoparticle assemblies, Nanoscale **6**, 8984 (2014).

[42] C. Moularas, Y. Georgiou, K. Adamska, and Y. Deligiannakis, Thermoplasmonic heat generation efficiency by nonmonodisperse core-shell $AgO@SiO_2$ nanoparticle ensemble, J. Phys. Chem. C **123**, 22499 (2019).

[43] V. Siahpoush, S. Ahmadi-kandjani, and A. Nikniazi, Effect of plasmonic coupling on photothermal behavior of random nanoparticles, Opt. Commun. **420**, 52 (2018).

[44] A. O. Govorov, W. Zhang, T. Skeini, H. Richardson, J. Lee, and N. A. Kotov, Gold nanoparticle ensembles as heaters and actuators: Melting and collective plasmon resonances, Nanoscale Res. Lett. **1**, 84 (2006).

[45] L. X. Ma and C. C. Wang, Isosbestic light absorption by metallic dimers: Effect of interparticle electromagnetic coupling, Appl. Opt. **59**, 1028 (2020).

[46] Y. T. Ren, Q. Chen, H. Qi, L. M. Ruan, and J. M. Dai, Phase transition induced by localized surface plasmon resonance of nanoparticle assemblies, Int. J. Heat Mass Transfer **127**, 244 (2018).

[47] K. Metwally, S. Mensah, and G. Baffou, Isosbestic thermoplasmonic nanostructures, ACS Photonics **4**, 1544 (2017).

[48] P. O. Chapuis, M. Laroche, S. Volz, and J.-J. Greffet, Radiative heat transfer between metallic nanoparticles, Appl. Phys. Lett. **92**, 201906 (2008).

[49] P. Ben-Abdallah, R. Messina, S.-A. Biehs, M. Tschikin, K. Joulain, and C. Henkel, Heat Superdiffusion in Plasmonic Nanostructure Networks, Phys. Rev. Lett. **111**, 174301 (2013).

[50] V. Yannopapas and N. V. Vitanov, Spatiotemporal Control of Temperature in Nanostructures Heated by Coherent Laser Fields, Phys. Rev. Lett. **110**, 044302 (2013).

[51] A. Rajabpour, R. Seif, S. Arabha, M. M. Heyhat, S. Merabia, and A. Hassanali, Thermal transport at a nanoparticle-water interface: A molecular dynamics and continuum modeling study, J. Chem. Phys. **150**, 114701 (2019).

[52] M. M. Aksoy, M. AlHosani, and Y. Bayazitoglu, Thermal resistance for Au-water and Ag-water interfaces: Molecular dynamics simulations, Int. J. Thermophys. **42**, 87 (2021).

[53] M. Roodbari, M. Abbasi, S. Arabha, A. Gharedaghi, and A. Rajabpour, Interfacial thermal conductance between TiO_2 nanoparticle and water: A molecular dynamics study, J. Mol. Liq. **348**, 118053 (2022).

[54] J. Vera and Y. Bayazitoglu, Temperature and heat flux dependence of thermal resistance of water/metal nanoparticle interfaces at sub-boiling temperatures, Int. J. Heat Mass Transfer **86**, 433 (2015).

[55] J. Alper and K. Hamad-Schifferli, Effect of ligands on thermal dissipation from gold nanorods, Langmuir **26**, 3786 (2010).

[56] E. Palik, *Handbook of Optical Constants of Solids* (Academic, New York, 1998).

[57] J. H. Hodak, I. Martini, and G. V. Hartland, Spectroscopy and dynamics of nanometer-sized noble metal particles, J. Phys. Chem. B **102**, 6958 (1998).

[58] M. G. Luo, J. M. Zhao, L. H. Liu, B. Guizal, and M. Antezza, Many-body effective thermal conductivity in phase-change nanoparticle chains due to near-field radiative heat transfer, Int. J. Heat Mass Transfer **166**, 120793 (2021).

[59] P. Ben-Abdallah, S.-A. Biehs, and K. Joulain, Many-Body Radiative Heat Transfer Theory, Phys. Rev. Lett. **107**, 114301 (2011).

[60] J. Dong, J. M. Zhao, and L. H. Liu, Radiative heat transfer in many-body systems: Coupled electric and magnetic dipole approach, Phys. Rev. B **95**, 125411 (2017).

[61] P. Ben-Abdallah, Multitip Near-Field Scanning Thermal Microscopy, Phys. Rev. Lett. **123**, 264301 (2019).

[62] S. L. Zou and G. C. Schatz, Narrow plasmonic/photonic extinction and scattering line shapes for one and two dimensional silver nanoparticle arrays, J. Chem. Phys. **121**, 12606 (2004).